

Chapter 1

2D NUMERICAL SIMULATION OF STELLAR CONVECTION

An Overview

Matthias Steffen *

Astrophysikalisches Institut Potsdam, An der Sternwarte 16, D-14482 Potsdam, Germany

msteffen@aip.de

Abstract The dynamics and thermal structure of the surface layers of stars with outer convection zones can be studied in some detail by means of numerical simulations of time-dependent compressible convection. In an effort to investigate the properties of “stellar granulation” as a function of spectral type, we have carried out elaborate 2-dimensional radiation hydrodynamics calculations of surface convection for a variety of stellar parameters. The main features of these simulations are reviewed, with particular reference to standard mixing length models.

1. INTRODUCTION

Convection is a universal feature. Essentially all types of stars have either a convective core, a convective envelope, or both. Low-mass stars are fully convective, giants may accommodate several distinct convective shells. In the case of the Sun, the energy transport in the inner parts is entirely due to radiation, while in the outer 28.7% (in radius) it is primarily due to large-scale convective currents. At the surface, the solar granulation is the visible imprint of gas flows in the outermost layers of the convection zone.

The role of stellar convection is far-reaching: Convective energy transport determines the internal temperature structure of a star and its ra-

*Institut für Theoretische Physik und Astrophysik, Universität Kiel, D-24098 Kiel, Germany

dius (which decreases with increasing convective efficiency), and hence controls the star’s global properties. Convective regions are chemically completely mixed, and overshooting convective flows lead to partial mixing of the adjacent radiative layers. “Overshoot” and similar mixing processes which are not confined to the convectively unstable regions are thought to be responsible for the existence of carbon stars, carbon-rich white dwarfs, and for the destruction of lithium in solar-type stars. Convective motions and concomitant temperature fluctuations exert a direct influence on stellar spectra, causing small but practically relevant changes in wavelength position, shape and strength of spectral lines. The stochastic convective motions can excite stellar oscillations (like in the Sun) and are a source of acoustic energy, contributing to the heating of stellar chromospheres. Finally, convection and rotation are necessary preconditions for the operation of the magnetic dynamo mechanism, and hence for stellar activity.

Unfortunately, a closed analytical theory of stellar convection is lacking due to the complexity of the underlying hydrodynamical problem. So far, stellar structure models still rely on a phenomenological approximation, the so-called *mixing-length theory* (MLT).

2. HYDRODYNAMICAL MODELING

The differential equations governing the physics of stellar convection are well-known but difficult to solve: the conservation equations of hydrodynamics, coupled with the equations of radiative energy transfer. While their highly non-linear and non-local character precludes an adequate analytical treatment, the numerical integration of the system of partial differential equations is now feasible. This approach constitutes an increasingly powerful method to study in detail the time-dependent properties of a radiating, partially ionized fluid under stellar conditions. Using modern supercomputers, it is possible to perform 3D numerical simulations of stellar (surface) convection with realistic background physics. But even 2D convection models require substantial amounts of computer time, particularly for solving the radiative transfer problem.

Just like “classical” stellar atmospheres, the hydrodynamical models are characterized by effective temperature, T_{eff} , surface gravity, g , and chemical composition of the plasma. But in contrast to the mixing-length models, there is no longer any free parameter to adjust the efficiency of the convective energy transport. Based on first principles, radiation hydrodynamics (RHD) simulations provide physically consistent *ab initio* models of stellar convection which can serve to check the validity of MLT.

3. STATE-OF-THE-ART RESULTS

In the following, we present some results of elaborate 2-dimensional RHD simulations of solar and stellar surface convection. The models comprise small sections near the stellar surface, typically extending over 10 pressure scale height in vertical direction, including the photosphere, the thermal boundary layer near optical depth $\tau_{\text{Ross}} = 1$, and parts of the subphotospheric layers. For the hotter stars of type A and early F, the surface convection zone(s) are shallow enough to be entirely fitted into the computational box. For the cooler, solar-like stars, only the uppermost layers of the deep convection zones can be included into the model, requiring an open lower boundary.

These simulations are designed to resolve the “stellar granulation”. The effect of the smaller scales, which cannot be resolved numerically, is modeled by means of a subgrid scale viscosity (so-called Large Eddy Simulation approach). Spatial scales larger than the computational box are ignored. We employ a realistic equation of state, accounting for ionization of H, HeI, HeII and H₂ molecule formation. In order to avoid problematic approximations (like the diffusion or Eddington approximation), we solve the non-local radiative transfer problem along a large number ($\approx 10\,000$) of rays in a number of wavelength bands, with realistic opacities including the influence of spectral lines. For further details see Ludwig et al. (1994) and Freytag et al. (1996).

3.1 SOLAR-TYPE SURFACE CONVECTION

A grid of about 60 simulation runs of solar-type surface convection, covering the range $4\,300\text{ K} \leq T_{\text{eff}} \leq 7\,100\text{ K}$; $2.54 \leq \log g \leq 4.74$ (solar metallicity), is presently available. In general, the hydrodynamical simulations exhibit *unsteady convective flows* and superimposed *oscillations*.

3.1.1 General properties. The basic features of the numerical convection models are illustrated in Fig. 1.1, showing a representative snapshot from a well-relaxed simulation of the solar granulation. In the convectively unstable, subphotospheric layers, fast ($v \lesssim c_s$) narrow downdrafts (also called plumes or jets) stand out as the most prominent feature. They are embedded in broad ascending regions (the granules) where velocities are significantly lower. We find enormous temperature differences between the cool downflows and the hot upflows ($\Delta T_{\text{max}} \approx 5\,000\text{ K}$ at $z \approx -100\text{ km}$ in the solar case). Near optical depth $\tau = 1$, efficient radiative surface cooling produces a very thin thermal boundary layer over the ascending parts of the flow, where the temperature drops sharply with height and the gas density exhibits a local inversion.

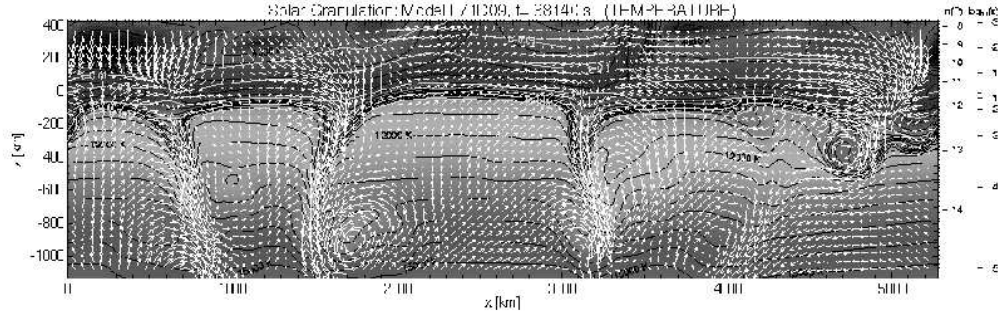


Figure 1.1 Representative snapshot from a 2-dimensional numerical simulation of solar surface convection after 38 140 s of simulated time. This model was computed on a Cartesian grid with 210×106 mesh points (tick marks along upper and right side), with periodic lateral boundary conditions ($L = 5\,250$ km). “Open” boundary conditions at the bottom and top of the computational domain are designed to minimize artificial distortions of the flow. The velocity field is represented by pseudo streamlines, indicating the displacement of a test particle over 20 sec (maximum velocity is 10.1 km/s at this moment); the temperature structure is outlined by temperature contours in steps of 500 K. Geometrical height $z = 0$ (scale at left) corresponds to $\tau_{\text{Ross}} \approx 1$; scales at right refer to the horizontally averaged gas pressure [dyn cm^{-2}] and Rosseland optical depth τ_{Ross} .

Although convectively stable according to the Schwarzschild criterion, the photosphere ($\tau \lesssim 1$) is by no means static. Convective flows overshooting into the stable layers from below are decelerated here and deflected sideways. This can sometimes result in transonic horizontal streams which lead to the formation of shocks in the vicinity of strong downdrafts (see vertical fronts in Fig. 1.1 near $x = 3\,400$ km, $z \gtrsim 200$ km). Oscillations excited by the stochastic convective motions contribute to the photospheric velocity field as well. Interestingly, the oscillation periods lie in the range 150 to 500 s for the solar simulation, in close agreements with the observed 5 minute oscillations. Controlled by the balance between dynamical cooling (due to adiabatic expansion) and radiative heating (in the spectral lines), the photospheric temperature stratification is not at all plane-parallel. At least for the Sun, the resulting average temperature in the photosphere is slightly cooler than in radiative equilibrium.

A typical sequence of events seen in the time-dependent simulations is the formation of new downdrafts, their horizontal advection, and finally their merging with another downdraft, as illustrated in Fig. 1.2. We found that merging of downdrafts is a major source of acoustic energy flux. Fig. 1.2 also demonstrates the strong correlation between vertical convective velocity and emergent continuum intensity. Downdrafts are clearly seen as narrow dark regions in intensity. On the other hand,

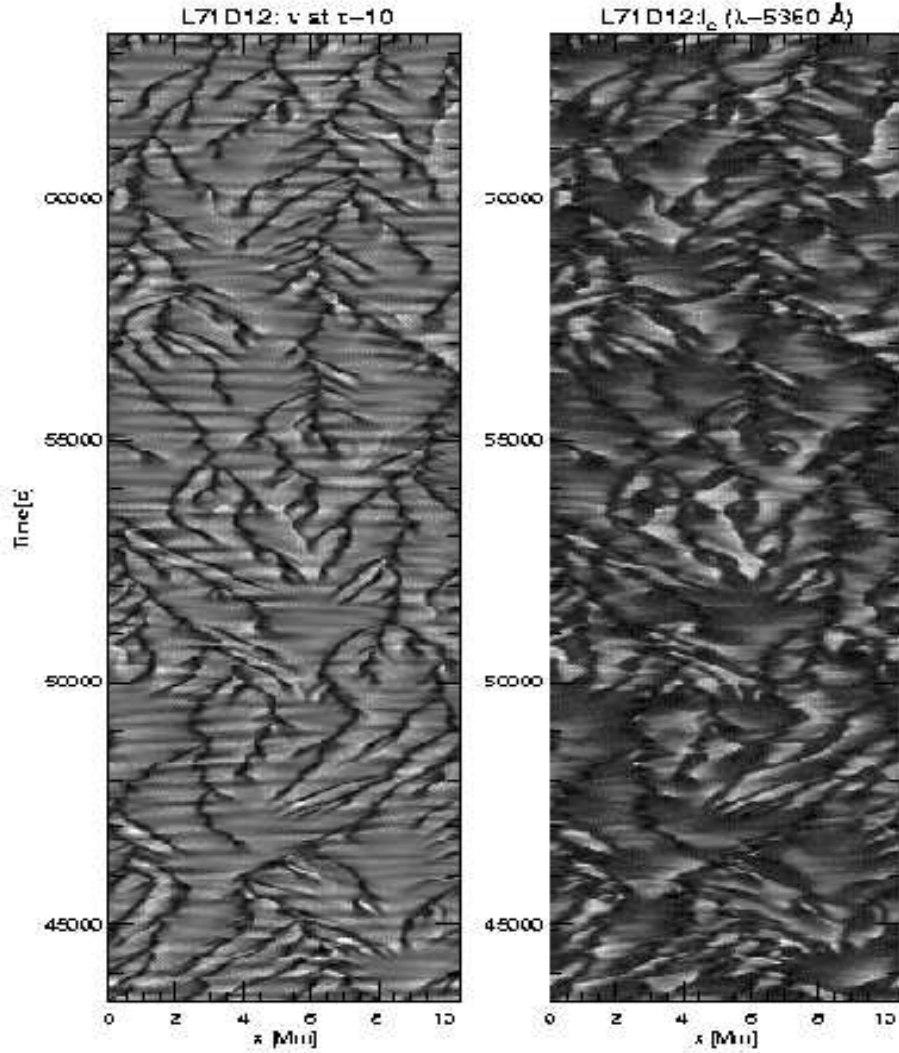


Figure 1.2 Grey-scale plot of vertical velocity at $\tau_{\text{Ross}} \approx 10$ (left) and emergent continuum intensity at $\lambda 5380 \text{ \AA}$ (right) as a function of horizontal position and time. Dark shades indicate downward velocities and low intensities, respectively. Note that the signature of superimposed “5 min oscillations” is clearly seen in both maps. Data were taken from a solar simulation that is similar to the one shown in Fig. 1.1 but has twice the horizontal size (420x106 grid).

the correlation is not perfect: in the ascending regions there is more structure in the intensity data than in velocity. Small “granules” tend to be brighter than large ones, which often show the highest intensity

at their edges. Indeed, the power spectra of velocity and intensity differ significantly; the p-modes stand out much more clearly in velocity power.

3.1.2 Comparison with MLT. The numerical simulations contain a wealth of information and may be analyzed in various ways. For comparison with mixing-length theory, we have averaged the quantities of interest horizontally (over planes of constant geometrical height or over surfaces of constant optical depth) and over time. Overshoot into the photosphere is substantial according to the hydrodynamical models (Fig. 1.3). Due to the local nature of MLT, however, it is suppressed in the mixing-length models. But even in the unstable layers it is impossible to adjust the mixing-length parameter α such as to reproduce the average 2D or 3D velocity field in the framework of MLT. The situation is similar for the thermal structure $T(\tau)$ (not shown). The difference between the 2D and the 3D simulation results is probably related to the higher acoustic activity of the 2D models (Ludwig & Nordlund, this volume).

The turbulent pressure P_{turb} amounts to a significant fraction of the gas pressure in the solar atmosphere (bottom panel of Fig. 1.3) and hence affects the geometric scale of the surface layers. Due to the lack of overshoot and the uncertainty in the proper choice of α , mixing-length models fail to account for the correct distribution of the turbulent pressure, often even assuming $P_{\text{turb}} = 0$.

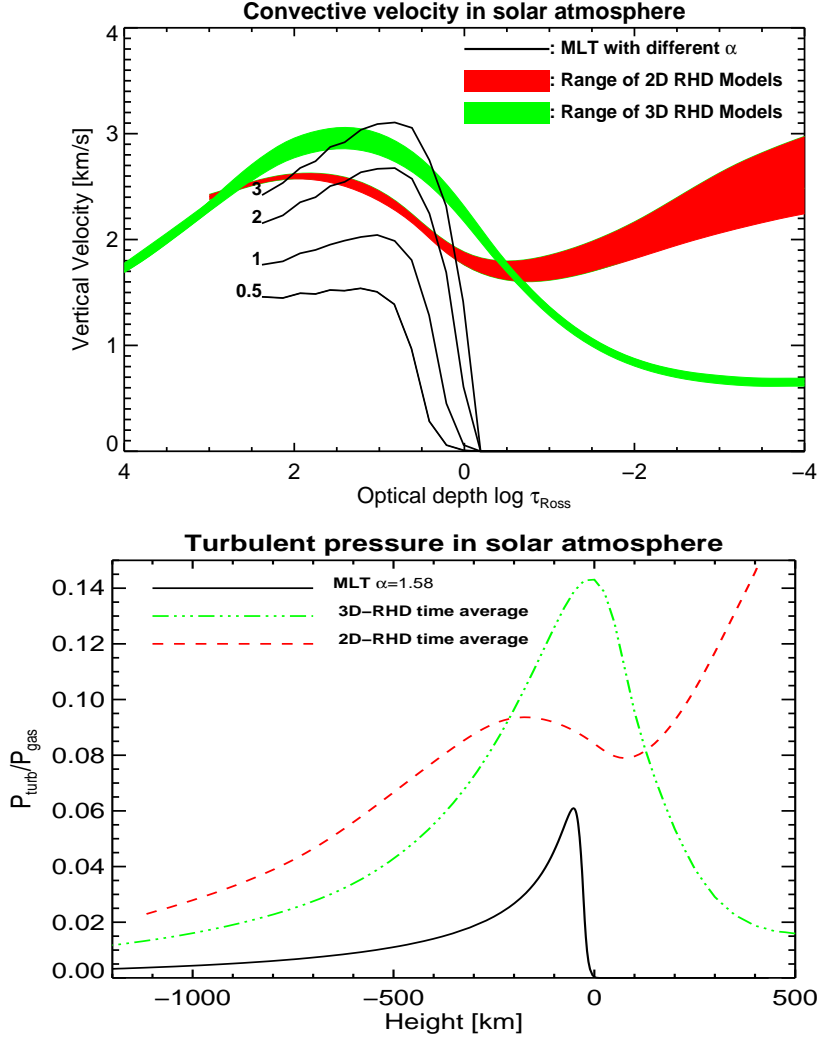


Figure 1.3 Top: Vertical convective velocity v as a function of optical depth τ_{Ross} as obtained from standard MLT ($\alpha = 0.5, 1, 2, 3$) compared with v_{rms} derived from 2D and 3D numerical simulations by averaging over planes of constant τ_{Ross} and over time. **Bottom:** Ratio of turbulent pressure ρv^2 to gas pressure P as a function of geometrical height as obtained from MLT for $\alpha = 1.58$ (adequate for evolution calculations) compared with the results obtained from 2D and 3D numerical simulations by averaging ρv^2 and P over horizontal planes and over time. Note that a self-consistent MLT solution does not exist. Rather, we obtained the plotted results *a posteriori* from a standard model computed without the effect of turbulent pressure according to the formalism by Böhm-Vitense (1958), using a non-grey $T(\tau)$ relation that is consistent with the numerical simulations. The 3D simulation results are courtesy of H.-G. Ludwig (see Ludwig & Nordlund, this volume).

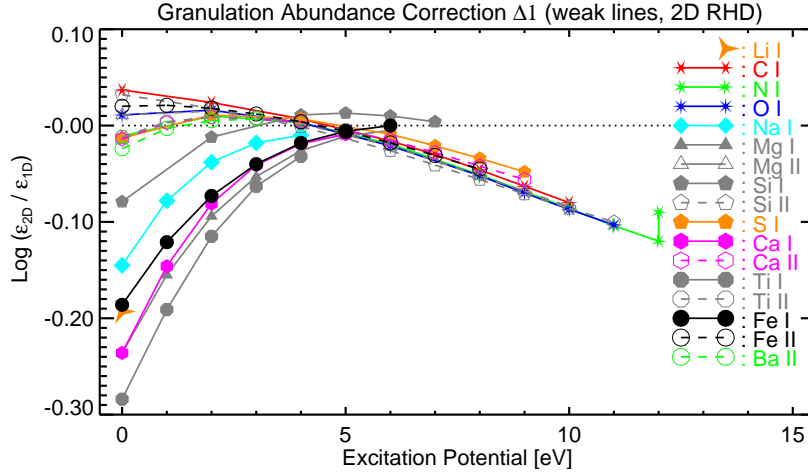


Figure 1.4 Logarithmic abundance correction to be applied to standard spectroscopic determinations of solar chemical abundances in order to compensate for the effects of photospheric temperature inhomogeneities. These “granulation corrections” depend in a systematic way on the excitation potential of the spectral line’s lower level and on the ionization potential of the atom or ion being considered. Corrections are valid for weak lines at $\lambda 5500 \text{ \AA}$. The Ni 12 eV line was also computed for $\lambda 10000 \text{ \AA}$ (upper symbol). In general, 5 eV lines are “safe”.

3.1.3 Spectral line formation. It is not surprising that the photospheric velocity field and temperature inhomogeneities due to convective overshoot affect the formation of spectral lines. We have computed LTE synthetic profiles for a set of weak ($W_\lambda < 10 \text{ m\AA}$) fictitious lines ($\lambda = 5500 \text{ \AA}$) of different elements and ions, based on an ensemble of representative snapshots from the 2D solar simulation. For each snapshot, we compared the equivalent width of the horizontally averaged line profile, $W_{2D} = \langle W_\lambda(\text{RHD}) \rangle$, with the equivalent width of the same line computed from the averaged (on τ -surfaces) RHD model, $W_{1D} = W_\lambda(\langle \text{RHD} \rangle)$. Averaged over all snapshots, the ratio W_{1D}/W_{2D} gives the correction factor that has to be applied to standard 1D abundance determinations in order to correct for the influence of photospheric inhomogeneities. The current results for a variety of different lines are summarized in Fig. 1.4. According to this investigation, lines of neutral minority species originating from the ground state are most affected. In the most extreme example, the standard analysis based on 0 eV Ti I lines would overestimate the titanium abundance by a factor of 2. The effects may be even larger for F-type stars!

3.1.4 Calibration of Mixing-Length Theory. As we have seen, the mean dynamical and thermal structure of the superadiabatic stellar

surface layers is systematically different in RHD and MLT models, respectively. In this sense, there is no way to establish a unique calibration of MLT by means of hydrodynamical simulations. However, it is possible to match particular properties by adjusting α . For stellar evolution, the key quantity is the entropy jump, Δs^* , from the surface to the interior. Based on our grid of solar-type RHD models, we have calibrated MLT by matching the quantity Δs^* , which can be “measured” from the simulations. This calibration yields the correct adiabat and depth of the convective envelope, and hence the appropriate $\alpha^*(T_{\text{eff}}, \log g)$ for stellar evolution calculations. To our knowledge, it is the first theoretical prediction of how the mixing-length parameter varies across (parts of) the Hertzsprung-Russell diagram (for details see Ludwig, Freytag & Steffen 1999).

For the Sun, the result is $\alpha^*(2\text{D RHD}) \approx 1.61 \pm 0.05$ and $\alpha^*(3\text{D RHD}) \approx 1.68 \pm 0.05$, in excellent agreement with the helioseismic value of $\alpha^*(\text{Helios.}) \approx 1.71 \pm 0.02$. In the covered range of stellar parameters, we find that α^* depends primarily on T_{eff} and varies systematically between about 1.3 for F dwarfs and 1.8 for K subgiants. Certainly, the fact that α^* varies only moderately with stellar type is one of the reasons for the surprising success of MLT over the past 40 years.

3.2 CONVECTION IN A-TYPE STARS

Our grid of hydrodynamical models of A and early F main sequence stars comprises about 30 simulation runs in the range $7\,200\text{ K} \leq T_{\text{eff}} \leq 9\,500\text{ K}$; $\log g = 4.44$. These type of stars exhibit two distinct convection zones: the one at the surface is driven by the combined first ionization of hydrogen and helium, the deeper one is related to the second ionization of helium. In the example shown in Fig. 1.5, the Schwarzschild-unstable regions are separated by a stable radiative layer of about two pressure scale heights. Nevertheless, the hydrodynamical simulations indicate that the two convection zones are effectively connected by vigorous currents and that the stable buffer layer is completely mixed, in contrast to MLT predictions.

A closer inspection of the simulation data showed that the velocity field due to overshooting convective motions declines exponentially with distance from the Schwarzschild boundary (in the example of Fig. 1.5, the velocity scale height below the HeII convection zone is $H_v \approx 0.35 H_p$). We found that mixing due to overshoot can be described as a diffusion process, with a diffusion coefficient $D \sim v_{\text{rms}}^2$. For a slightly hotter star ($T_{\text{eff}} = 7943\text{ K}$, $\log g = 4.34$) we have shown that the convectively mixed

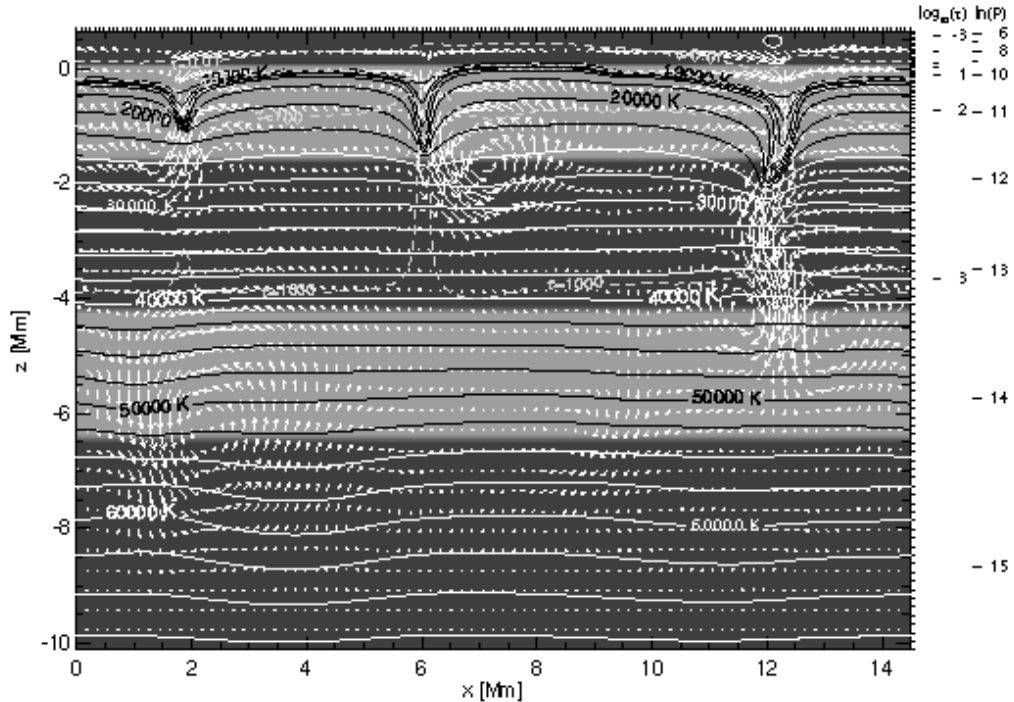


Figure 1.5 Snapshot from a 2D simulation of convection in an A8 main sequence star ($T_{\text{eff}} = 7600$ K, $\log g = 4.4$ [cgs units]) with 2 distinct convection zones. The unstable regions ($d\bar{s}/dz < 0$, where \bar{s} is the horizontally averaged specific entropy) are shaded light gray. The velocity field is represented by pseudo streamlines, indicating the displacement of a test particle over 40 sec (maximum velocity is 19.0 km/s at this moment); the temperature structure is outlined by temperature contours in steps of 2500 K. Dashed lines trace levels of constant $\tau = 0.01, 1, 100, 1000$. Located in the lower radiative zone, a closed lower boundary is appropriate. Grid size 182x95.

mass is underestimated by a factor of 10 if overshoot is ignored (Freytag, Ludwig & Steffen 1996).

In stellar structure models, overshoot is usually implemented by specifying the distance ($d_{\text{over}} = \delta H_p$) by which the convection zone proper is extended due to “penetration” into the stable layers. This empirical approach ignores the hydrodynamical results indicating that overshoot is characterized by an exponential velocity field and (partial) diffusive mixing.

4. CONCLUSIONS

Radiation hydrodynamics simulations of stellar surface convection have now reached a level of sophistication far beyond idealized numerical

experiments. They are the key for a better understanding of the thermal structure and dynamics of stellar convection zones, including overshoot and its role for mixing.

The comparison with “classical” mixing-length models reveals quantitative and qualitative differences. In the simulations, the dynamics of convection is dominated by fast, cool, narrow downdrafts, which form coherent structures extending over many pressure scale heights. A pronounced up/down asymmetry is a general feature of the numerical models (2D as well as 3D), seen for all types of stars investigated so far. Obviously, this result is in stark contrast with the symmetric picture of MLT where “bubbles” are assumed to travel for about one pressure scale height before dissolving. Since the “jets” are driven by radiative cooling at the stellar surface, convection is an extremely non-local process. The properties of the surface determine the dynamics and structure of the whole convection zone. Certainly, the assumption of locality is a major problem with MLT.

Hydrodynamical model atmospheres can be used to study the formation of spectral lines in an inhomogeneous medium. For the Sun, we found that “granulation corrections” for spectroscopic abundance determinations can amount to -0.3 dex for the most temperature sensitive lines. These corrections are much larger than the well-known NLTE corrections that have been investigated so far. Work is under way to check whether these findings have notable consequences for the currently adopted chemical composition of the Sun and other stars.

While it seems hopeless to successfully model the structure of the superadiabatic surface layers within the framework of MLT, it is possible to calibrate MLT through hydrodynamical simulations for application to stellar evolution. Based on 2D radiation hydrodynamics, our present calibration ultimately needs to be verified by 3D simulations. In the meantime, we are working to extend the calibration to metal-poor stars, down to $[M/H]=-2$.

The hydrodynamical simulations for A-type stars (and White Dwarfs) demonstrate that the velocity field due to overshooting convective motions declines exponentially with distance from the Schwarzschild boundary and leads to diffusive mixing. Although this result is not directly applicable to strongly adiabatic conditions, we believe that the exponential depth-dependence of the diffusion coefficient is a general feature of overshoot and may have important implications for mixing and nucleosynthesis in stellar interiors.

Acknowledgments

The author is grateful to H.-G. Ludwig for making available some of his 3D simulation results and for computing MLT reference models. B. Freytag computed the A-star model and helped with processing the simulation data.

References

- Böhm-Vitense, E. (1958), *Z. Astrophys.* 46, 108
Freytag, B., Ludwig, H.-G., Steffen, M. (1996), *Astron. Astrophys.* 313, 497
Ludwig, H.-G., Jordan, S., Steffen, M. (1994), *Astron. Astrophys.* 284, 105
Ludwig, H.-G., Freytag, B., Steffen, M. (1999), *Astron. Astrophys.* 346, 111